Springer

Journal of
Mechanical
Science and
Technology

Journal of Mechanical Science and Technology 23 (2009) 2008~2021

www.springerlink.com/content/1738-494x
DOI 10.1007/s12206-009-0519-9

Free vibration analysis of functionally graded coupled circular plate with piezoelectric layers

S. Jafari Mehrabadi[1,*], M. H. Kargarnovin[2] and M. M. Najafizadeh[3]

[1]*Department of Mechanical Engineering, Islamic Azad University, Science and Research Branch of Tehran, Iran*
[2]*Department of Mechanical Engineering, Sharif University of Technology, Tehran, Iran*
[3]*Department of Mechanical Engineering, Azad University, Arak Branch, Iran*

(Manuscript Received December 12, 2007; Revised May 25, 2008; Accepted April 1, 2009)

Abstract

Based on classical plate theory (CLPT), free vibration analysis of a circular plate composed of functionally graded material (FGM) with its upper and lower surfaces bounded by two piezoelectric layers was performed. Assuming that the material properties vary in a power law manner within the thickness of the plate the governing differential equations are derived. The distribution of electric potential along the thickness direction in piezoelectric layers is considered to vary quadratically such that the Maxwell static electricity equation is satisfied. Then these equations are solved analytically for two different boundary conditions, namely clamped and simply supported edges. The validity of our analytical solution was checked by comparing the obtained resonant frequencies with those of an isotropic host plate. Furthermore, for both FGM plate and FGM plate with piezoelectric layers, natural frequencies were obtained by finite element method. Very good agreement was observed between the results of finite element method and the method presented in this paper. Then for the two aforementioned types of boundary conditions, the values of power index were changed and its effect on the resonant frequencies was studied. Also, the effect of piezoelectric thickness layers on the natural frequencies of FGM piezoelectric plate was investigated.

Keywords: Functionally Graded; Circular Plate; Piezoelectric; Vibration

1. Introduction

It is for some time that piezoelectric materials have found their way extensively and efficiently as an actuator or sensor in the vibration analysis of structural systems. They are usually used as embedded layers on the surfaces of different parts of any vibrating structure. In 1987 [1] in an analytic and experimental study, the piezoelectric actuators were used in intelligent structures comprised of a laminated composite plate bonded with segmented piezoelectric actuators. For such plates the static and dynamical models are obtained for segmented piezoelectric actuators that are either bonded on an elastic substructure or embedded in a laminated composite plate. In particular, one of the main branches of such study in the vibration of the structures is referred to as the vibration control of the plates.

In [2] the nonaxisymmetric vibration modes for a piezoelectric annular plate are described; also, reference [3] presents a finite element modeling of piezoelectric sensors and actuators using classical laminate plate theory. Furthermore, [4] investigated the modeling of piezoelectric rotary ultrasonic motors for predicting a prior performance as a function of design parameters using the Raleigh-Ritz assumed mode energy method. Reference [5] presents exact solution for static behavior of laminated piezoelectric plates with simply supported boundary conditions as stresses and displacement and electric potential de-

† This paper was recommended for publication in revised form by Associate Editor Seockhyun Kim
*Corresponding author. Tel.: +98 8614451352, Fax.: +98 861 3288444
E-mail address: sjmamir@gmail.com

rived.

In 1997 [6] worked on the dynamic of an annular piezoelectric motor stator. this paper details the study of an annular plate composed of one stainless steel lamina and either one or two piezoelectric laminates. [7, 8] have demonstrated a simple model for the free vibration of stator disk and an improved model using the finite difference and Ritz methods, for the free vibration of a disk with non-uniform thickness.

Most laminated structures are modeled as a collection of layers with specific material properties and several approaches to modeling these structures are possible, such as classical lamination theory [9, 10], first order and higher order shear deformation theories with or without rotary inertia [11, 12]. Moreover, a relatively unique and complex procedure by [13] and [14] are representative of common solution techniques. In [15], based on the three-dimensional elasticity theory, the axisymmetric state space formulation of piezoelectric laminated circular plates is derived, and results compared with those of finite element method.

In the dynamic analysis of circular layered plates, primarily [16-17] published a number of papers in the vibration of circular single layer plate. The analytical solution for free vibration of piezoelectric coupled moderately thick circular plates using Mindlin's plate theory for isotropic host plate is given in [18]. The objective of study in paper [19] is to present an approximate analytical one-term Galerkin solution for the problem of nonlinear deflection, thermal buckling and natural frequencies of a three-layer thin circular plate made of an isotropic elastic core with piezoelectric layers bonded to its faces. Also, in 2005 [20] studied the free vibration analysis of piezoelectric coupled annular plate using the Kirchhoff and Mindlin plate models.

In all the above-mentioned references the materials are isotropic, but in the recent years there have been many researches about FG material related to this paper, some of which will be introduced here.

In 2001, [21] analyzed out of displacement and stress field in a piezoelectric plate with functionally graded microstructure. Also, [22] investigated the nonlinear vibration of functionally graded plates with imperfection sensitivity so that equations of motion were derived with attention to initial stress and geometric imperfection size, and solved using perturbation technique, Galerkin method and Runge-Kutta method. In [23] an inverse problem of a functionally graded material for elliptical plate with large deflections based on the classical nonlinear Von Karman plate theory is presented. In [24] by using finite element analysis the asymmetric free vibration and thermoelastic stability of FGM circular plates are analyzed with due regard to field-consistency principle.

Reference [25] investigates large amplitude vibration and analyzes pre-stressed functionally graded material in laminated plates that are composed of a shear deformable functionally graded layer with two surface- mounted piezoelectric actuator layers. The nonlinear governing differential equations of motion for such system are derived by using Reddy's higher-order shear deformation plate theory. Also, [26] studied the free vibration of an isotropic circular plate with two piezoelectric layers mounted on the top and bottom surfaces of the plate.

In the present work the free vibration of an FGM plate patched with two full size piezoelectric layers on the top and the bottom of the plate is investigated. The physical and mechanical properties of the FGM plate are assumed to vary continuously through the thickness of the plate according to a simple power law function. Based on classical plate theory the governing differential equations of a thin coupled plate were derived. By using some mathematical techniques these differential equations are transformed to a sixth order ordinary differential equation, and finally by implementing the operator decomposition method on this equation, three Bessel type of equations are obtained which can easily be solved for the plate deflection and consequently the potential function. Having on hand the deflection of the plate and the potential function of the piezoelectric layers, after imposing the plate boundary conditions, the resonant frequencies of the coupled structure are obtained. At the end, the effect of changing the values of power index and the thickness of the piezoelectric layers on the resonant frequencies of system are studied.

2. FG and piezoelectric materials

2.1 Functionally graded materials (FGM)

FG materials are typically made of a continuous mixture of two different materials such as ceramic and metal. Indeed, due to its low conductivity, the ceramic constituent of the FG material offers better resistivity against high temperature. The metallic part

of the constituent, on the other hand, prevents the mixture from any type of fracture caused by induced stresses due to high temperature gradient. From a manufacturing point of view, nowadays not only can FGM easily be produced but one can control even the variation of the FG constituents in a specific way. For example, in an FG material made of ceramic and metal mixture, if the volume fraction of the ceramic part is represented by V_c and the metallic part by V_m, we have:

$$V_m + V_c = 1 \tag{1}$$

Based on the power law distribution (Reddy and Praveen, 1998 [32]), the variation of V_c vs. thickness coordinate z placed at the middle of thickness, can be expressed as:

$$V_c = \left(\frac{z}{2h} + \frac{1}{2}\right)^k \qquad k \geq 0 \tag{2}$$

In which 2h is thickness of the plate and k is power index that takes values grater than or equal to zero. Note that the variation of both constituents of ceramic and metal is linear when k=1. Moreover, for the value of k=0, a fully ceramic plate is intended. We assume that the inhomogeneous material properties, such as the modulus of elasticity, E, the coefficient of thermal expansion, α, and density ρ change in the thickness direction z based on Voigt's rule over the whole range of the volume fraction (Whetherhold et al., 1996 [33]), while Poisson's ratio υ, is assumed to be constant in the thickness direction as:

$$\begin{aligned} E(z) &= E_c V_c + E_m(1 - V_c) \\ \alpha(z) &= \alpha_c V_c + \alpha_m(1 - V_c) \\ \rho(z) &= \rho_c V_c + \rho_m(1 - V_c) \\ \upsilon(z) &= \upsilon \end{aligned} \tag{3}$$

Where subscripts m and c refer to the metal and ceramic constituents, respectively. After substituting V_c from Eq. (2), into Eqs. (3), material properties of the FGM plate are determined in the power law form which is the same as those proposed by Reddy and Praveen (1998):

$$E(z) = (E_c - E_m)\left(\frac{z}{2h} + \frac{1}{2}\right)^k + E_m$$

$$\alpha(z) = (\alpha_c - \alpha_m)\left(\frac{z}{2h} + \frac{1}{2}\right)^k + \alpha_m$$

$$\rho(z) = (\rho_c - \rho_m)\left(\frac{z}{2h} + \frac{1}{2}\right)^k + \rho_m$$

$$\upsilon(z) = \upsilon \tag{4}$$

Contrary to the most of the published papers on the FGM plates, in this paper we choose an FGM plate with upper part of steel and the lower part as nickel, whereas there is no limitation in our analysis to select instead other types of materials. To model properly the above selected compound FG plate, we have to switch the subscript m with c in the Eqs. (3-4), and vice versa. In this way, when k=0 the FGM plate becomes a uniform steel plate.

2.2 Piezoelectric materials

A constitutive elasto-static relation for symmetry piezoelectric materials in Cartesian coordinate for two dimensional is given as follows [31]:

$$\sigma_i = c_{ki}\varepsilon_k - e_{ji}E_k \qquad i, j, k = 1, 2, 3 \tag{5}$$

In which σ_i and ε_k represent the stress and strain tensor components, respectively, and e_{ij} represent the permeability constant of piezoelectric material, and E_k indicates the components of the electric field. Also, c_{ki} is related to the matrix of modulus of elasticity.
Based on well-known assumptions of classical plate theory, Eq. (5), can be represented by [26]:

$$\begin{bmatrix} \sigma_{11} \\ \sigma_{22} \\ \sigma_{13} \end{bmatrix} = \begin{bmatrix} \overline{c}_{11}^E & \overline{c}_{12}^E & 0 \\ \overline{c}_{12}^E & \overline{c}_{11}^E & 0 \\ 0 & 0 & \overline{c}_{11}^E - \overline{c}_{12}^E \end{bmatrix} \begin{bmatrix} \varepsilon_{11} \\ \varepsilon_{22} \\ \varepsilon_{12} \end{bmatrix} - \begin{bmatrix} 0 & 0 & \overline{e}_{31} \\ 0 & 0 & \overline{e}_{31} \\ 0 & 0 & 0 \end{bmatrix} \begin{bmatrix} E_1 \\ E_2 \\ E_3 \end{bmatrix} \tag{6}$$

$\overline{c}_{ij}^E$ Are the reduced components of the symmetric piezoelectric stiffness matrix given as the following, and e_{31} is the reduced permeability coefficient of piezoelectric material and given as [26]:

$$\overline{c}_{11}^E = c_{11}^E - \frac{\left(c_{13}^E\right)^2}{c_{33}^E}$$

$$\overline{c}_{12}^E = c_{12}^E - \frac{\left(c_{13}^E\right)^2}{c_{33}^E}$$

$$\overline{e}_{31} = e_{31} - \frac{\left(c_{13}^E\right)}{c_{33}^E} e_{33}$$

The above relations c_{ij}^{E} are the components of the piezoelectric stiffness matrix, and e_{31}, e_{33} are the permeability of piezoelectric material.

Moreover, the electric displacement-strain relation for the symmetry piezoelectric material is given by [31]:

$$\begin{bmatrix} D_1 \\ D_2 \\ D_3 \end{bmatrix} = \begin{bmatrix} 0 & 0 & 0 \\ 0 & 0 & 0 \\ \overline{e}_{31} & \overline{e}_{31} & 0 \end{bmatrix} \begin{bmatrix} \varepsilon_{11} \\ \varepsilon_{22} \\ \varepsilon_{12} \end{bmatrix} + \begin{bmatrix} \overline{E}_{11} & 0 & 0 \\ 0 & \overline{E}_{11} & 0 \\ 0 & 0 & \overline{E}_{33} \end{bmatrix} \begin{bmatrix} E_1 \\ E_2 \\ E_2 \end{bmatrix} \tag{7}$$

D_i (i=1,2,3) represents the components of an electric displacement, E_{11},E_{33} are the symmetric reduced dielectric of piezoelectric layer and given by [26]:

$$\overline{E}_{11} = E_{11} \qquad \overline{E}_{33} = E_{33} + \frac{e_{33}^2}{c_{33}^E}$$

E_{11},E_{33} are the dielectric coefficients of piezoelectric material (permittivity). Note that in polar coordinate 1,2,3 transforms the r, θ and z, respectively.

3. Constitutive relations for an fgm plate and piezoelectric layers under an electric potential field

3.1 Strain and stress field in circular FGM plate based on classical plate theory

Usually, in the analysis of a circular plate when the ratio of the thickness to radius is less than 1/10, classical plate theory is used in which the effect of the shear deformation and the rotary of inertia are neglected. According to this theory, the most general form of displacement components in the plate is given by [27]:

$$u_z = u_z(r,\theta,t) = w(r,\theta,t) \tag{8}$$

$$u_r = u_r(r,\theta,t) = -z\frac{\partial u_z}{\partial r} \tag{9}$$

$$u_\theta = u_\theta(r,\theta,t) = -\frac{z}{r}\frac{\partial u_z}{\partial \theta} \tag{10}$$

Where u_z, u_r ,u_θ are displacements of the plate in the transverse, radial and tangential directions, respectively. Also, the poling direction of the piezoelectric material is assumed to be in the z direction. When an external electric potential is applied across the piezoelectric layer, different strain components as following are induced which result in bending of the plate [28]:

$$\varepsilon_{rr} = \frac{\partial u_r}{\partial r} = -z\frac{\partial^2 w}{\partial r^2} \tag{11}$$

$$\varepsilon_{\theta\theta} = \frac{1}{r}\frac{\partial u_\theta}{\partial \theta} + \frac{u_r}{r} = -z\left(\frac{1}{r^2}\frac{\partial^2 w}{\partial \theta^2} + \frac{1}{r}\frac{\partial w}{\partial r}\right) \tag{12}$$

$$\varepsilon_{r\theta} = \frac{1}{r}\frac{\partial u_\theta}{\partial \theta} + \frac{u_r}{r} = -z\left(\frac{1}{r^2}\frac{\partial^2 w}{\partial \theta^2} + \frac{1}{r}\frac{\partial w}{\partial r}\right) \tag{13}$$

In which ε_{rr} , $\varepsilon_{\theta\theta}$, $\varepsilon_{r\theta}$ are the radial, tangential and shear strains components, respectively.

Based on the generalized Hooke's Law, the stress components in terms displacement are [28]:

$$\sigma_{rr} = \frac{-Ez}{1-\upsilon^2}\left[\frac{\partial^2 w}{\partial r^2} + \upsilon\left(\frac{1}{r^2}\frac{\partial^2 w}{\partial \theta^2} + \frac{1}{r}\frac{\partial w}{\partial r}\right)\right] \tag{14}$$

$$\sigma_{\theta\theta} = \frac{-E\,z}{1-\upsilon^2}\left[\left(\frac{1}{r^2}\frac{\partial^2 w}{\partial \theta^2} + \frac{1}{r}\frac{\partial w}{\partial r} + \upsilon\frac{\partial^2 w}{\partial r^2}\right)\right] \tag{15}$$

$$\tau_{r\theta} = -\frac{Ez}{1+\upsilon}\left(\frac{1}{r}\frac{\partial^2 w}{\partial \theta \partial r} - \frac{1}{r^2}\frac{\partial w}{\partial \theta}\right) \tag{16}$$

E represents the modulus of elasticity of the FGM plate.

3.2 The electric potential, electric intensity, flux density and strain-stress relations in the piezoelectric layers

To determine the natural frequencies of a vibrating coupled plate, two piezoelectric layers are attached to the FG plate and they can be used as an actuator or sensor. There are several different models representing the input electric potential for such a piezoelectric layer. We decided to adopt the following Wang et al. electric potential, which is appropriate for free vibrations of the proposed system [26]:

$$\Phi(r,\theta,z,t) = \left[1 - \left(\frac{2z - 2h - h_1}{h_1}\right)^2\right]\varphi(r,\theta,t) \tag{17}$$

in which φ represent the function of the electric potential specifically for the mid-surface plane of the piezoelectric layer, z is measured from the middle plane of the plate in the global z-direction, h_1 ,2h and r_0 are the thickness of the piezoelectric layer, thick-

ness of the host circular plate and its radius, respectively.(see Fig. 1)

Based on the given form of the electric potential across the thickness direction Eq. (17), the components of electric field intensity, E_i and electric flux densities D_i , can be obtained as [30]:

$$E_r = -\frac{\partial \Phi}{\partial r} = -\left[1-\left(\frac{2z-2h-h_1}{h_1}\right)^2\right]\frac{\partial \varphi}{\partial r} \tag{18}$$

$$E_\theta = -\frac{1}{r}\frac{\partial \Phi}{\partial \theta} = -\frac{1}{r}\left[1-\left(\frac{2z-2h-h_1}{h_1}\right)^2\right]\frac{\partial \varphi}{\partial \theta} \tag{19}$$

$$E_z = -\frac{\partial \Phi}{\partial z} = \frac{4\left(2z-2h-h_1\right)}{h_1^2}\varphi \tag{20}$$

$$D_r = \overline{E}_{11}E_r = -\overline{E}_{11}\left[1-\left(\frac{2z-2h-h_1}{h_1}\right)^2\right]\frac{\partial \varphi}{\partial r} \tag{21}$$

$$D_\theta = \overline{E}_{11}E_\theta = -\frac{\overline{E}_{11}}{r}\left[1-\left(\frac{2z-2h-h_1}{h_1}\right)^2\right]\frac{\partial \varphi}{\partial \theta} \tag{22}$$

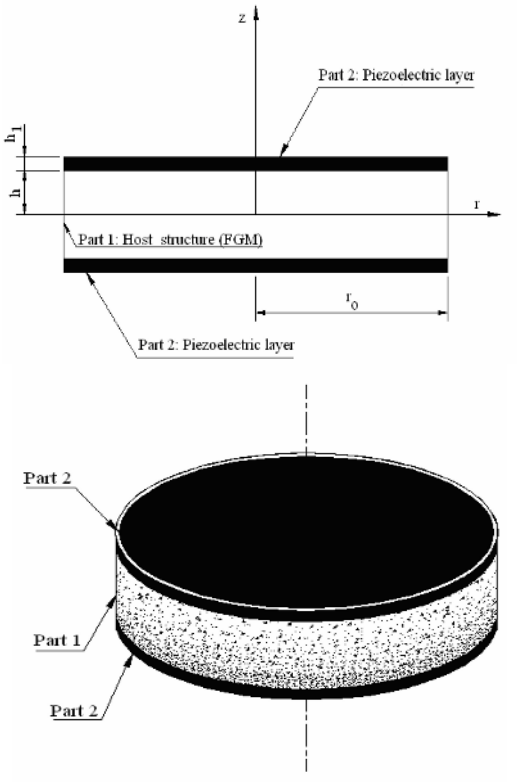

Fig. 1. Schematic representation of the FGM circular plate with two piezoelectric layers mounted on its upper and lower surfaces.

$$D_z = \overline{E}_{33}E_z + \overline{e}_{31}\left(\varepsilon_{rr}+\varepsilon_{\theta\theta}\right) = \frac{4\overline{E}_{33}\left(2z-2h-h_1\right)\varphi}{h_1^2} - \overline{e}_{31}z\Delta w \tag{23}$$

in which, E_r , E_θ , E_z are the electric field intensity in the r, θ and z directions, respectively. Also, D_r, D_θ and D_z are the corresponding electric displacements in indicated directions; Δ is the Laplace operator in the polar coordinate given by:

$$\Delta = \frac{\partial^2}{\partial r^2} + \frac{1}{r}\frac{\partial}{\partial r} + \frac{1}{r^2}\frac{\partial^2}{\partial \theta^2}$$

The stress – strain –electric field intensity relations in the piezoelectric layers in the polar coordinate referred to Eq. (6) can be written as [31]:

$$\sigma_{rr}^p = \overline{c}_{11}^p\varepsilon_{rr} + \overline{c}_{12}^p\varepsilon_{\theta\theta} - \overline{e}_{31}E_z \tag{24}$$

$$\sigma_{\theta\theta}^p = \overline{c}_{12}^p\varepsilon_{rr} + \overline{c}_{11}^p\varepsilon_{\theta\theta} - \overline{e}_{31}E_z \tag{25}$$

$$\tau_{r\theta}^p = \left(\overline{c}_{11}^p - \overline{c}_{12}^p\right)\varepsilon_{r\theta} \tag{26}$$

The superscript p indicates the parameter under consideration belongs to the piezoelectric layers. Because of continuity of piezoelectric layers and host plate, the strain displacements in both of them are similar.

4. Derivation of the governing differential equations of the coupled FGM circular plate

To obtain the governing differential equation of the couple circular plate, we begin with resultant moments as [27]:

$$\begin{aligned} M_{rr} &= \int_{-h}^{h} z\sigma_{rr}dz + 2\int_{h}^{h+h_1} z\sigma_{rr}^p dz \\ M_{\theta\theta} &= \int_{-h}^{h} z\sigma_{\theta\theta}dz + 2\int_{h}^{h+h_1} z\sigma_{\theta\theta}^p dz \\ M_{r\theta} &= \int_{-h}^{h} z\tau_{r\theta}dz + 2\int_{h}^{h+h_1} z\tau_{r\theta}^p dz \end{aligned} \tag{27}$$

Now by substituting the stress components in terms of displacement components Eqs. (14)-(16), and Eqs. (24)-(26), in Eqs. (27), and carrying out the integrations, one would get:

$$M_{rr} = -\left[\left(d_1+d_2\right)\frac{\partial^2 w}{\partial r^2} + \left(\upsilon d_1 + \frac{\overline{c}_{12}^p}{\overline{c}_{11}^p}d_2\right)\left(\frac{1}{r}\frac{\partial w}{\partial r} + \frac{1}{r^2}\frac{\partial^2 w}{\partial \theta^2}\right)\right] - \frac{4}{3}h_1\overline{e}_{31}\varphi$$

$$M_{\theta\theta} = -\left[(d_1 + d_2)\left(\frac{1}{r}\frac{\partial w}{\partial r} + \frac{1}{r^2}\frac{\partial^2 w}{\partial \theta^2} \right) + \left(\upsilon d_1 + \frac{\bar{c}_{12}^{p}}{\bar{c}_{11}^{p}} d_2 \right) \frac{\partial^2 w}{\partial r^2} \right]$$
$$-\frac{4}{3} h_1 \bar{e}_{31} \varphi$$
$$M_{r\theta} = -\left[(1-\upsilon) d_1 + \left(1 - \frac{\bar{c}_{12}^{p}}{\bar{c}_{11}^{p}} \right) d_2 \right] \left(\frac{1}{r}\frac{\partial^2 w}{\partial r \partial \theta} - \frac{1}{r^2}\frac{\partial w}{\partial \theta} \right) \tag{28}$$

Where the coefficients of d_1 and d_2 in the above equations are:

$$d_1 = \int_{-h}^{h} \frac{E_h z^2}{(1-\upsilon^2)} dz$$
$$d_2 = 2\int_{h}^{h+h_1} \bar{c}_{11}^{p} z^2 dz \tag{29}$$

Also, the resultant shear forces are given as [28]:

$$Q_r = \frac{\partial M_{rr}}{\partial r} + \frac{1}{r}\frac{\partial M_{r\theta}}{\partial \theta} + \frac{M_{rr} - M_{\theta\theta}}{r} \tag{30}$$

$$Q_\theta = \frac{\partial M_{r\theta}}{\partial r} + \frac{1}{r}\frac{\partial M_{r\theta}}{\partial \theta} + 2\frac{M_{r\theta}}{r} \tag{31}$$

The differential equation of motion in the z- direction based on the classical plate theory is [26]:

$$\frac{\partial Q_r}{\partial r} + \frac{1}{r}\frac{\partial Q_\theta}{\partial \theta} + \frac{Q_r}{r} = \int_{-h}^{h} \rho_h \frac{\partial^2 u_z}{\partial t^2} dz + 2\int_{h}^{h+h_1} \rho_p \frac{\partial^2 u_z}{\partial t^2} dz \tag{32}$$

Now, by substituting Eqs. (28), into Eqs. (30)-(31), and the results into Eq. (32), one would get:

$$(d_1 + d_2)\Delta\Delta w + \frac{4}{3} h_1 \bar{e}_{31} \Delta\varphi + 2(\rho_h h + \rho_p h_1)\frac{\partial^2 w}{\partial t^2} = 0 \tag{33}$$

in which ρ_h, and ρ_p are the material densities of the host plate and the piezoelectric layers, respectively.

Note that all of the electrical variables primarily must satisfy Maxwell's equation, which requires that the divergence of the electric flux density vanishes at any point within the media. This condition can be satisfied by enforcing the integration of the electric flux divergence across the thickness of the piezoelectric layers for any r and θ, [30]:

$$\int_{h}^{h+h_1} \vec{\nabla}.\vec{D} dz = 0 \tag{34}$$

The operator $\vec{\nabla}$ in the above equation is the gradient operator in the polar coordinate.
By substituting Eqs. (21-23), into the above equation, we arrive at:

$$\frac{h_1^2 \bar{E}_{11}}{12\bar{E}_{33}} \Delta\varphi - \varphi + \frac{h_1^2 \bar{e}_{31}}{8\bar{E}_{33}} \Delta w = 0 \tag{35}$$

5. Solving equations

Primarily, we solve Eqs. (33-35) simultaneously by which φ can be expressed in terms of w as:

$$\varphi(r,\theta,t) = -\frac{(d_1 + d_2) h_1 \bar{E}_{11}}{16\bar{e}_{31}\bar{E}_{33}} \Delta\Delta w + \frac{h_1^2 \bar{e}_{31}}{8\bar{E}_{33}} \Delta w -$$
$$\frac{h_1(\rho_p h_1 + \rho_h h)}{8\bar{e}_{31}\bar{E}_{33}} \frac{\partial^2 w}{\partial t^2} \tag{36}$$

By applying the operator Δ to the above equation one gets:

$$\Delta\varphi(r,\theta,t) = -\frac{(d_1 + d_2) h_1 \bar{E}_{11}}{16\bar{e}_{31}\bar{E}_{33}} \Delta\Delta\Delta w + \frac{h_1^2 \bar{e}_{31}}{8\bar{E}_{33}} \Delta\Delta w -$$
$$\frac{h_1(\rho_p h_1 + \rho_h h)\bar{E}_{11}}{8\bar{e}_{31}\bar{E}_{33}} \Delta\left(\frac{\partial^2 w}{\partial t^2} \right) \tag{37}$$

Substituting Eq. (37) into Eq. (33) results in a decoupled six-order partial differential equation as:

$$P_3\Delta\Delta\Delta w - P_2\Delta\Delta w + P_1\Delta\left(\frac{\partial^2 w}{\partial t^2} \right) - P_0 \frac{\partial^2 w}{\partial t^2} = 0 \tag{38}$$

The coefficients of P_0, P_1,P_2, P_3 are:

$$P_0 = 2(\rho_h h + \rho_p h_1) \qquad P_1 = \frac{h_1^2 \bar{E}_{11}}{12\bar{E}_{33}}(\rho_h h + \rho_p h_1) \tag{39}$$

$$P_2 = d_1 + d_2 + \frac{h_1^3 \bar{e}_{31}^2}{6\bar{E}_{33}} \qquad P_3 = \frac{h_1^2 \bar{E}_{11}}{12\bar{E}_{33}}(d_1 + d_2) \tag{40}$$

For solving the w and φ we first assume that

$$w(r,\theta,t) = w_1(r) e^{i(m\theta - \omega t)} \tag{41}$$

where $w_1(r)$ is the amplitude of the z- direction displacement as a function of radial displacement only; ω is the natural angular frequency of the compound plate; and m is the wave number in the circumferen-

tial direction. Rewriting Eq. (38), in terms of $w_1(r)$ and by using of Eq. (41), with canceling the $e^{i(m\theta-\omega t)}$ term, gives a differential equation, namely:

$$P_3\overline{\Delta\Delta\Delta}w_1 - P_2\overline{\Delta\Delta}w_1 - \omega^2 P_1\overline{\Delta}w_1 + \omega^2 P_0 w_1 = 0 \tag{42}$$

Where, the operator $\overline{\Delta}$ is given by:

$$\overline{\Delta} = \frac{d^2}{dr^2} + \frac{1}{r}\frac{d}{dr} - \frac{m^2}{r^2}$$

With solving the Eq. (42), by method of decomposition operator and in view of the non-singularity of w_1 at the center of the plate, the solution of Eq. (42), can be written as:

$$w_1(r) = A_{1m}Z_{1m}(\alpha_1 r) + A_{2m}Z_{2m}(\alpha_2 r) + A_{3m}Z_{3m}(\alpha_3 r) \tag{43}$$

Where:

$$\alpha_1 = \sqrt{|x_1|} \qquad \alpha_2 = \sqrt{|x_2|} \qquad \alpha_3 = \sqrt{|x_3|} \tag{44}$$

and x_1, x_2, x_3 are the roots of the following cubic characteristic equation:

$$P_3 x^3 - P_2 x^2 - \omega^2 P_1 x + \omega^2 P_0 = 0 \tag{45}$$

and:

$$Z_{im}(\alpha_i r) = Z_{im}(\alpha_i, r) = \begin{Bmatrix} J_m(\alpha_{ir}) & x_i \prec 0 \\ I_m(\alpha_{ir}) & x_i \succ 0 \end{Bmatrix} \quad i = 1,2,3 \tag{46}$$

Here, $J_m(\alpha_{ir})$ is the first Bessel function and $I_m(\alpha_{ir})$ is the modified first type Bessel function of order m.

For solution of φ, we assume:

$$\varphi(r,\theta,t) = \varphi_1(r)e^{i(m\theta-\omega t)} \tag{47}$$

Then we calculate $\overline{\Delta}\, w_1$, $\overline{\Delta\Delta}\, w_1$ and from Eq. (43), as below:

$$\overline{\Delta}w_1 = A_{1m}s_1\alpha_1^{\,2}Z_{1p}(\alpha_1 r) + A_{2m}s_2\alpha_2^{\,2}Z_{2m}(\alpha_2 r) + A_{3m}s_3\alpha_3^{\,2}Z_{3m}(\alpha_3 r) \tag{48}$$

$$\overline{\Delta\Delta}w_1 = A_{1m}\alpha_1^{\,4}Z_{1m}(\alpha_1 r) + A_{2m}\alpha_2^{\,4}Z_{2m}(\alpha_2 r) + A_{3m}\alpha_3^{\,4}Z_{3m}(\alpha_3 r) \tag{49}$$

where s_i (i=1, 2,3) are the signs of x_i (i=1,2,3) respectively. Now by substituting Eqs. (41-43)- (47), into Eq. (36), we find below a relation for φ_1:

$$\begin{aligned}\varphi_1(r) = {} & \left\{A_{1m}h_1\left[2s_1\alpha_1^{\,2}h_1\bar{e}_{31}^{\,2} - (d_1+d_2)\alpha_1^{\,4}\bar{E}_{11} + 2(\rho_h h + \rho_p h_1)\omega^2\bar{E}_{11}\right]\right\}\left(\frac{z_{1m}(\alpha_1 r)}{16\bar{e}_{31}\bar{E}_{33}}\right) \\ & + \left\{A_{2m}h_1\left[2s_2\alpha_2^{\,2}h_1\bar{e}_{31}^{\,2} - (d_1+d_2)\alpha_2^{\,4}\bar{E}_{11} + 2(\rho_h h + \rho_p h_1)\omega^2\bar{E}_{11}\right]\right\}\left(\frac{z_{2m}(\alpha_2 r)}{16\bar{e}_{31}\bar{E}_{33}}\right) \\ & + \left\{A_{3m}h_1\left[2s_3\alpha_3^{\,2}h_1\bar{e}_{31}^{\,2} - (d_1+d_2)\alpha_3^{\,4}\bar{E}_{11} + 2(\rho_h h + \rho_p h_1)\omega^2\bar{E}_{11}\right]\right\}\left(\frac{z_{3m}(\alpha_3 r)}{16\bar{e}_{31}\bar{E}_{33}}\right)\end{aligned} \tag{50}$$

6. Case studies, results and discussions

To obtain explicitly the natural frequencies of the compound solid FGM circular plate, we consider the following two different kinds of boundary conditions: clamped and simply supported.

The FG (steel-nickel) material is selected such that it is easier for us to compare the obtained results in this study with other existing ones. The material properties and geometry size of the FGM plate and piezoelectric layers which have been used in both cases are listed in Table 1.

Table 1. Material properties and geometric size of the piezoelectric FGM plate [26-35].

Property	Host structure (FG material)		Piezoelectric layer (PZT4)
	Steel:	Nickle:	
E (Gpa)	200	205	$C_{11}^E = 132$(Gpa)
			$C_{12}^E = 71$(Gpa)
			$C_{13}^E = 73$(Gpa)
			$C_{33}^E = 115$(Gpa)
Density (Kg/m^3)	7800	8900	7.5×10^3
$e_{31}(cm)^{-2}$			-4.1
$e_{33}(cm)^{-2}$			14.1
$e_{11}(Fm)^{-2}$			7.124×10^{-9}
r_o(mm)			600
h(mm)			10
h_1(mm)			2

6.1 Clamped circular compound plate

In this case the boundary conditions are:

$$\left(w = \frac{dw}{dr} = \frac{d\varphi}{dr} \right)_{r=r_0} = 0 \tag{51}$$

After imposing above boundary conditions on Eqs. (41, 47), By using of Eqs. (43, 50), the characteristic equation can be obtained as:

$$\begin{vmatrix} c_{11} & c_{12} & c_{13} \\ c_{21} & c_{22} & c_{23} \\ c_{31} & c_{32} & c_{33} \end{vmatrix} = 0 \tag{52}$$

where:

$$c_{11} = z_{1m}(\alpha_1 r_0) \qquad c_{12} = z_{2m}(\alpha_2 r_0)$$
$$c_{13} = z_{3m}(\alpha_3 r_0) \tag{53}$$

$$c_{21} = \alpha_1 r_0 z'_{1m}(\alpha_1 r_0) \qquad c_{22} = \alpha_2 r_0 z'_{2m}(\alpha_2 r_0)$$
$$c_{23} = \alpha_3 r_0 z'_{3m}(\alpha_3 r_0) \tag{54}$$

$$c_{31} = \left[\frac{h_1^2 r_0 s_1 \alpha_1^3}{8} - \frac{(d_1+d_2) h_1 r_0 \alpha_1^5 \bar{E}_{11}}{16 \bar{e}_{31}^2} + \frac{(d_1+d_2) h_1 \alpha_1 \lambda^4 \bar{E}_{11}}{16 \bar{e}_{31}^2 r_0^3} \right] z'_{1m}(\alpha_1 r_0)$$

$$c_{32} = \left[\frac{h_1^2 r_0 s_2 \alpha_2^3}{8} - \frac{(d_1+d_2) h_1 r_0 \alpha_2^5 \bar{E}_{11}}{16 \bar{e}_{31}^2} + \frac{(d_1+d_2) h_1 \alpha_2 \lambda^4 \bar{E}_{11}}{16 \bar{e}_{31}^2 r_0^3} \right] z'_{2m}(\alpha_2 r_0) \tag{55}$$

$$c_{33} = \left[\frac{h_1^2 r_0 s_3 \alpha_3^3}{8} - \frac{(d_1+d_2) h_1 r_0 \alpha_3^5 \bar{E}_{11}}{16 \bar{e}_{31}^2} + \frac{(d_1+d_2) h_1 \alpha_3 \lambda^4 \bar{E}_{11}}{16 \bar{e}_{31}^2 r_0^3} \right] z'_{3m}(\alpha_3 r_0)$$

$$\lambda = r_0 \left[\frac{2(\rho_h h + \rho_p h_1)\omega^2}{(d_1+d_2)} \right]^{\frac{1}{4}} \tag{56}$$

In the above equations the $(')$ symbol indicates the derivative with respect to r, and λ is the nondimensional angular natural frequency.

After calculating ω from Eq. (52), and using Eqs. (43, 50, 51), we find the mode shape of w_1 as:

$$w_1(r) = A_{3m} \{ [\alpha_3 z_{2m}(\alpha_2 r_0) z'_{3m}(\alpha_3 r_0) - \alpha_2 z_{3m}(\alpha_3 r_0) z'_{2m}(\alpha_2 r_0)\ ][\alpha_2 z_{1m}(\alpha_1 r_0) z'_{2m}(\alpha_2 r_0) - \alpha_1 z_{2m}(\alpha_2 r_0) z'_{1m}(\alpha_1 r_0)\ ]^{-1} z_{1m}(\alpha_1 r) \} + [\alpha_1 z_{3m}(\alpha_3 r_0) z'_{1m}(\alpha_1 r_0) - \alpha_3 z_{1m}(\alpha_1 r_0) z'_{3m}(\alpha_3 r_0)\ ][\alpha_2 z_{1m}(\alpha_1 r_0) z'_{2m}(\alpha_2 r_0) - \alpha_1 z_{2m}(\alpha_2 r_0) z'_{1m}(\alpha_1 r_0)\ ]^{-1} z_{2m}(\alpha_2 r) + z_{3m}(\alpha_3 r)\ \} \tag{57}$$

And, by using Eqs. (43, 50, 51), we have the electric potential as:

$$\varphi_1(r) = A_{3m} \{ [\alpha_3 z_{2m}(\alpha_2 r_0) z'_{3m}(\alpha_3 r_0) - \alpha_2 z_{3m}(\alpha_3 r_0) z'_{2m}(\alpha_2 r_0)\ ][\alpha_2 z_{1m}(\alpha_1 r_0) z'_{2m}(\alpha_2 r_0) - (16 \bar{e}_{31} \bar{E}_{33})\ ]^{-1} z_{1m}(\alpha_1 r) + [\alpha_1 z_{3m}(\alpha_3 r_0) z'_{1m}(\alpha_1 r_0) - \alpha_3 z_{1m}(\alpha_1 r_0) z'_{3m}(\alpha_3 r_0)\ ][\alpha_2 z_{1m}(16 \bar{e}_{31} \bar{E}_{33})\ ]^{-1} z_{2m}(\alpha_2 r)\ \} \tag{58}$$

Before going further into the discussion of the obtained numerical results, we have to make sure that the obtained results are valid. To do this, initially for some special cases, results are compared with those given in the literature [26, 28, 29]. In the next step, since there were no published results for the compound piezoelectric FGM plate, we decided to verify the validity of the obtained results with those of FEM results. Our FEM model for piezo-FG plate consists of a 3D 6-noded solid element with the number of total nodes 40106, number of total elements 36855, and 6 DOF per node.

For this case, i.e., clamped plate, Table 2 shows the numerical results of our method compared with other references and techniques.

6.2 Simply supported compound circular plate

In this case the boundary conditions are:

$$\left(w = (M_{rr}) = \frac{d\varphi}{dr} \right)_{r=r_0} = 0 \tag{59}$$

After imposing above boundary equations on Eqs. (41, 43, 28, 50), the characteristic equation can be obtained as:

$$\begin{vmatrix} s_{11} & s_{12} & s_{13} \\ s_{21} & s_{22} & s_{23} \\ s_{31} & s_{32} & s_{32} \end{vmatrix} = 0 \tag{60}$$

Table 2. Values of the first three natural frequencies for FGM plate and piezo-FGM plate in the case of clamped boundary condition for various values of power index and mode number.

Power Index	FGM plate-f(Hz)			
Mode No.	Piezo-FGM plate-f(Hz)			
k m	Present (analytic)	Present (FEM)	Error (%)	Wang etal. [26]
0 0	138.41 143.63	139.29 144.46	0.64 0.58	138.48 143.71
0 1	288.05 298.92	289.80 300.22	0.61 0.43	288.20 299.07
0 2	472.55 490.37	473.48 491.8	0.20 0.29	472.79 490.62
1 0	134.63 140.26	135.47 141.05	0.62 0.56	- -
1 1	280.17 291.89	281.86 293.14	0.60 0.43	- -
1 2	459.62 478.84	460.49 480.21	0.19 0.29	- -
3 0	132.70 138.54	133.68 139.46	0.74 0.66	- -
3 1	276.19 288.33	278.14 289.83	0.71 0.52	- -
3 2	453.09 472.99	454.42 474.79	0.29 0.38	- -
5 0	132.12 138.01	133.11 138.94	0.75 0.67	- -
5 1	274.96 287.21	276.95 288.75	0.72 0.54	- -
5 2	451.06 471.16	452.47 473.04	0.31 0.40	- -
7 0	131.85 137.76	132.83 138.69	0.74 0.68	- -
7 1	274.39 286.69	276.36 288.22	0.72 0.53	- -
7 2	450.13 470.31	451.51 472.17	0.31 0.40	- -
9 0	131.69 137.62	132.75 138.54	0.80 0.67	- -
9 1	274.07 286.4	276.20 287.91	0.78 0.53	- -
9 2	449.60 469.83	450.90 471.65	0.29 0.39	- -
10 0	131.64 137.57	132.60 138.48	0.73 0.66	- -
10 1	273.96 286.3	275.89 287.79	0.70 0.52	- -
10 2	449.42 469.66	450.74 471.46	0.29 0.38	- -

The coefficients of s_{ij} are:

$$
\begin{aligned}
&s_{11} = z_{1m}(\alpha_1 r_0)\\
&s_{12} = z_{2m}(\alpha_2 r_0)\\
&s_{13} = z_{3m}(\alpha_3 r_0)
\end{aligned}
\tag{61}
$$

$$
\begin{aligned}
&s_{21} = \alpha_1^{\,2}(d_1+d_3)z''_{1m}(\alpha_1 r_0) + \frac{\alpha_1}{r}\left(\upsilon d_1 + \frac{\bar{c}_{12}}{\bar{c}_{11}}d_2\right)\\
&+\left\{\left(\frac{-m^2}{r^2}\right)\left(\upsilon d_1 + \frac{\bar{c}_{12}}{\bar{c}_{11}}d_2\right) + \left(\frac{h_1}{12\bar{E}_{11}}\right)\left[2s_1 h_1^{\,2}\alpha_1^{\,2}\bar{e}_{31}^{\,2}\right.\right.\\
&\left.\left.-(d_1+d_2)h_1\alpha_1^{\,4}\bar{E}_{11} + 2\omega^2\bar{E}_{11}h_1(\rho_p h_1 + \rho_h h)\right]\right\}\\
&z_{1m}(\alpha_1 r_0)\\
&s_{22} = \alpha_2^{\,2}(d_1+d_3)z''_{2m}(\alpha_2 r_0) + \frac{\alpha_2}{r}\left(\upsilon d_1 + \frac{\bar{c}_{12}}{\bar{c}_{11}}d_2\right)\\
&+\left\{\left(\frac{-m^2}{r^2}\right)\left(\upsilon d_1 + \frac{\bar{c}_{12}}{\bar{c}_{11}}d_2\right) + \left(\frac{h_1}{12\bar{E}_{11}}\right)\left[2s_2 h_1^{\,2}\alpha_2^{\,2}\bar{e}_{31}^{\,2}\right.\right.\\
&\left.\left.-(d_1+d_2)h_1\alpha_2^{\,4}\bar{E}_{11} + 2\omega^2\bar{E}_{11}h_1(\rho_p h_1 + \rho_h h)\right]\right\}\\
&z_{2m}(\alpha_2 r_0)\\
&s_{23} = \alpha_3^{\,2}(d_1+d_3)z''_{3m}(\alpha_3 r_0) + \frac{\alpha_3}{r}\left(\upsilon d_1 + \frac{\bar{c}_{12}}{\bar{c}_{11}}d_2\right)\\
&+\left\{\left(\frac{-m^2}{r^2}\right)\left(\upsilon d_1 + \frac{\bar{c}_{12}}{\bar{c}_{11}}d_2\right) + \left(\frac{h_1}{12\bar{E}_{11}}\right)\left[2s_3 h_1^{\,2}\alpha_3^{\,2}\bar{e}_{31}^{\,2}\right.\right.\\
&\left.\left.-(d_1+d_2)h_1\alpha_3^{\,4}\bar{E}_{11} + 2\omega^2\bar{E}_{11}h_1(\rho_p h_1 + \rho_h h)\right]\right\}\\
&z_{3m}(\alpha_3 r_0)
\end{aligned}
\tag{62}
$$

$$
\begin{aligned}
&s_{31} = \left[\frac{h_1 r_0 s_1 \alpha_1^{\,3}}{8} - \frac{(d_1+d_2)h_1 r_0 \alpha_1^{\,5}\bar{E}_{11}}{16\bar{e}_{31}^{\,2}} +\right.\\
&\left.\frac{(d_1+d_2)h_1\alpha_1\lambda^4\bar{E}_{11}}{16\bar{e}_{31}^{\,2}r_0}\right]z'_{1m}(\alpha_1 r_0)\\
&s_{32} = \left[\frac{h_1 r_0 s_2 \alpha_2^{\,3}}{8} - \frac{(d_1+d_2)h_1 r_0 \alpha_2^{\,5}\bar{E}_{11}}{16\bar{e}_{31}^{\,2}} +\right.\\
&\left.\frac{(d_1+d_2)h_1\alpha_2\lambda^4\bar{E}_{11}}{16\bar{e}_{31}^{\,2}r_0}\right]z'_{2m}(\alpha_2 r_0)\\
&s_{33} = \left[\frac{h_1 r_0 s_3 \alpha_3^{\,3}}{8} - \frac{(d_1+d_2)h_1 r_0 \alpha_3^{\,5}\bar{E}_{11}}{16\bar{e}_{31}^{\,2}} +\right.\\
&\left.\frac{(d_1+d_2)h_1\alpha_3\lambda^4\bar{E}_{11}}{16\bar{e}_{31}^{\,2}r_0}\right]z'_{3m}(\alpha_3 r_0)
\end{aligned}
\tag{63}
$$

Also, in this case after calculating ω or λ from Eq. (60), and using Eqs. 41, 43, 59 w_1 can be obtained in terms of A_{3m} as:

$$w_1(r) = A_{3m}\left[\frac{s_{13}s_{22}-s_{12}s_{23}}{s_{12}s_{21}-s_{11}s_{22}} z_{1m}(\alpha_{1m}r) + \frac{s_{11}s_{23}-s_{13}s_{21}}{s_{12}s_{21}-s_{11}s_{22}} z_{2m}(\alpha_{2m}r) + z_{3m}(\alpha_{3m}r)\right] \quad (64)$$

By aid of Eqs. 28, 43, 50, 59 and following the same procedure, the function φ_1 can be calculated.

Note that the mode shapes of the w_1, and φ_1 relation become different for different boundary conditions because their related characteristic equations are different, as given in Eqs. (52), and (60).

For this case, i.e., simply supported plate, Table 3 shows the numerical results of our method compared with other references and techniques.

As we can see from Tables 2 and 3, the obtained results from the analytical method when k=0 (isotropic steel plate) correspond closely with the results of references [26-28] and FEM solution. As it is seen in these tables, the maximum estimated error of our solution with FEM is about 0.80% for the simply support clamped case.

The obtained results in these tables indicate that by increasing the value of k, the frequency of system decreases for both types of boundary conditions in all different vibrational modes. Moreover, this decreasing trend of frequency for smaller values of k is more pronounced, for example, in the case of clamped plate by increasing k from 1 to 3 (about 200%) the frequency of the first mode for the compound plate decreases by 1.23%, but by increasing k from 3 to 9 (about 200%) of the same plate and for the same mode, the frequency decreases by 0.66%. It is also observed that for the FGM plate in the case of simply supported boundary condition by increasing k from 0 to 3 the frequency decreases in the third mode of vibration about 4.12%, but by increasing k from 5 to 10, the frequency decreases for the same plate and the same mode is about 0.36%. To see better the effect of k variations on the natural frequencies of the different plates, Figs. 2-5 also illustrate these variations only for the first and third mode shapes.

As it is seen from Figs. 2-5, the behavior of the system follows the same trend in all different cases, i.e., the natural frequencies of the system decrease by increasing of k and do not change considerably for k values greater than 7. In fact, the FGM plate becomes a nickel plate and compound plate transforms to a laminated plate with nickel core as a host plate.

Table 3. Values of the first three natural frequencies for FGM plate and piezo FGM-plate in the case of simply supported boundary condition for various values of power index and mode number.

Power Index	FGM plate-f(Hz)			
Mode No.	Piezo-FGM plate-f(Hz)			
k *m*	Present (analytic)	Present (FEM)	Error (%)	Wang etal. [26]
0 0	66.86 69.33	67.27 69.61	0.61 0.41	- 69.37
0 1	188.31 195.36	189.58 195.75	0.67 0.20	- 195.46
0 2	347.04 360.07	349.36 360.14	0.67 0.02	- 360.26
1 0	65.03 67.69	65.37 67.97	0.52 0.41	- -
1 1	183.16 190.76	184.38 191.20	0.67 0.23	- -
1 2	337.46 351.62	339.78 351.65	0.69 0.01	- -
3 0	64.11 66.88	64.51 67.20	0.62 0.48	- -
3 1	180.55 188.42	181.95 188.98	0.78 0.30	- -
3 2	332.75 347.32	335.31 347.68	0.77 0.10	- -
5 0	63.82 66.62	64.23 66.95	0.64 0.50	- -
5 1	179.75 187.72	181.17 188.28	0.79 0.30	- -
5 2	331.25 345.97	333.87 346.39	0.79 0.12	- -
7 0	63.69 66.53	64.09 66.83	0.63 0.45	- -
7 1	179.37 187.37	180.79 187.93	0.79 0.30	- -
7 2	330.56 345.35	333.15 345.76	0.78 0.12	- -
9 0	63.62 66.43	64.01 66.76	0.61 0.49	- -
9 1	179.16 187.18	180.55 187.73	0.78 0.29	- -
9 2	330.18 345.00	332.82 345.38	0.80 0.11	- -
10 0	187.18 66.40	187.73 66.73	0.29 0.49	- -
10 1	179.10 187.12	180.48 187.65	0.77 0.28	- -
10 2	330.06 344.87	332.59 345.24	0.77 0.11	- -

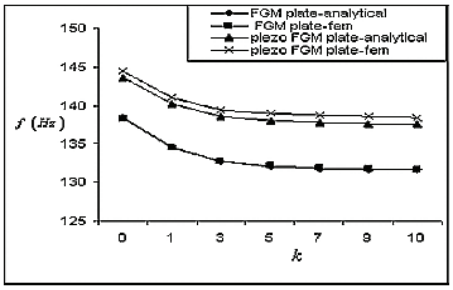

Fig. 2. Effect of power index on the natural frequency for the case of clamped boundary condition (first mode).

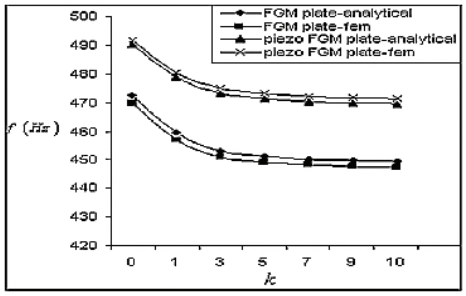

Fig. 3. Effect of power index on the natural frequency for the case of clamped boundary condition (third mode).

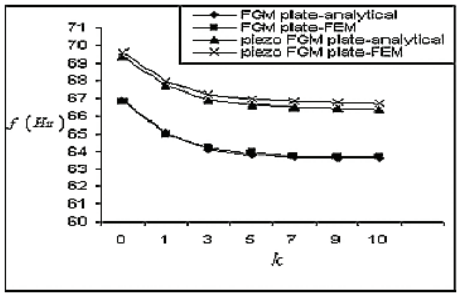

Fig. 4. Effect of power index on the natural frequency for the case of simply supported boundary condition (first mode).

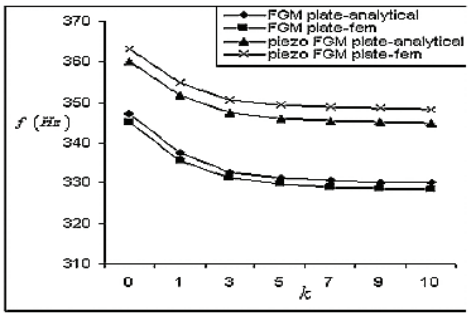

Fig. 5. Effect of power index on the natural frequency for the case of simply supported boundary condition (third mode).

6.3 The effect of piezoelectric thickness on the natural frequencies of simply supported compound plate

Based on the derived relations for the case of simply supported circular compound plate, the natural frequencies of the same plate were calculated in which the thickness of the FGM core was kept fixed and the thickness of the piezoelectric layers varied such that $h_1/2h=1/12, 1/10, 1/8, 1/5$. The obtained results of such changes for first and third modes are given in Figs. 6-7.

The obtained results reveal that by increasing the aspect ratio of $h_1/2h$, the natural frequency of laminated plate increases for all values of k. However, for a fixed value of aspect ratio, as it was shown in the previous tables, increasing of k will cause a decrease in the value of natural frequencies.

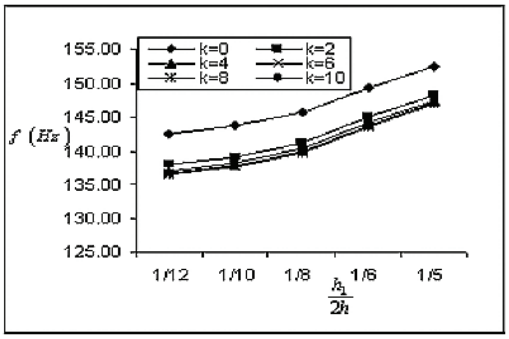

Fig. 6. Effect of piezo layer thickness on the natural frequency for simply supported boundary condition-(first mode).

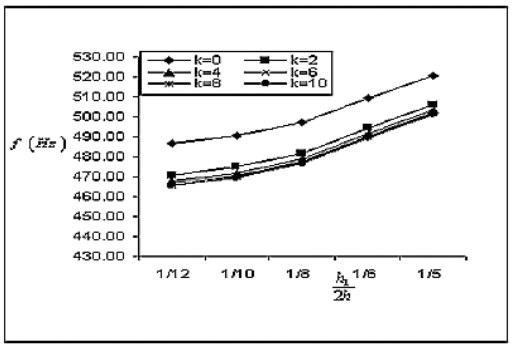

Fig. 7. Effect of piezo layer thickness on the natural frequency for simply supported boundary condition-(third mode).

6.4 The effect of piezoelectric thickness on the natural frequency of clamped compound plate

Based on the derived relations for the case of a clamped circular compound plate, the natural frequencies of the same plate were calculated in which the thickness of the FGM core was kept fixed and the thickness of the piezoelectric layers varied such that $h_1/2h$=1/12, 1/10, 1/8, 1/6, 1/5. The obtained results of such changes are given in Table 4 (note that for summary purposes, the table results are shown for the cases of $h_1/2h$=1/12, 1/8).

Regarding the obtained results in Table 4, we can say that by increasing the aspect ratio of $h_1/2h$, the natural frequency of the laminated plate increases for all values of k. However, for a fixed value of aspect ratio, as it was shown in the previous tables, increasing of k will cause a decrease in the value of natural frequencies. Moreover, as it was stated before, variation of the natural frequency is more sensitive for smaller values of k.

To get a better insight out of the quoted results in Table 4, on a selective base the results for the first and third natural frequencies are presented in Figs. 8-9.

Finally, the variation of the first natural frequency of simply supported and clamped circular FGM plate with and without piezoelectric layers vs. aspect ratio, r_0/h, when k=0 (i.e., isotropic plate) is presented in Fig. 10, Note that, for brevity, the related table of such results is not given here.

Generally, Fig. 10 shows that the first natural frequency of the clamped (with or without piezoelectric layers) is higher than the simply supported ones for all values of r_0/h. Furthermore, for high values of r_0/h the first natural frequency approaches to an almost constant value. In addition, the effect of piezoelectric layers on the natural frequency is more pronounced for small values of r_0/h for either of the boundary conditions.

Lastly, the effect of r_0/h variation on the first natural frequency of a clamped compound plate for different values of power index is shown in Fig. 10; again here for brevity, the obtained results in a table form are not given.

Moreover, Fig. 10 shows that the first natural frequency of the compound clamped plate decreases as r_0/h increases. Furthermore, for high values of r_0/h the first natural frequency approaches to an almost constant value, no matter how much would be the value of power index. In addition, the effect of power index on the natural frequency is more pronounced for small values of r_0/h.

Table 4. The first three natural frequencies of the clamped compound plate for different values of power index and aspect ratios of $h_1/2h$=1/12, 1/8.

$h_1/2h$	k m	f(Hz)	$h_1/2h$	k m	f(Hz)
1/12	0 0	68.79	1/8	0 0	70.25
	0 1	193.79		0 1	197.98
	0 2	357.18		0 2	364.91
	2 0	66.56		2 0	68.11
	2 1	187.53		2 1	191.94
	2 2	345.65		2 2	353.78
	4 0	66.13		4 0	67.69
	4 1	186.31		4 1	190.75
	4 2	343.39		4 2	351.59
	6 0	65.95		6 0	67.52
	6 1	185.82		6 1	190.28
	6 2	342.49		6 2	350.72
	8 0	65.87		8 0	67.43
	8 1	185.57		8 1	190.03
	8 2	342.03		8 2	350.26
	10 0	65.81		10 0	67.38
	10 1	185.42		10 1	189.88
	10 2	341.75		10 2	349.99

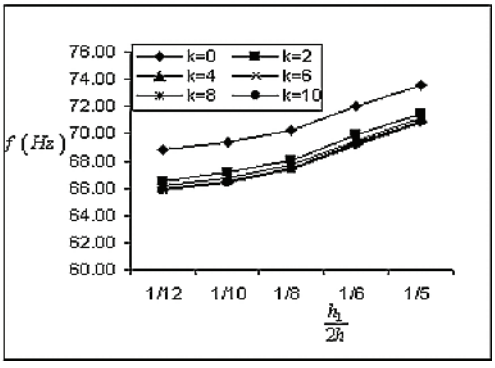

Fig. 8. Effect of piezo layer thickness on the natural frequency-clamped supported boundary condition-(first mode).

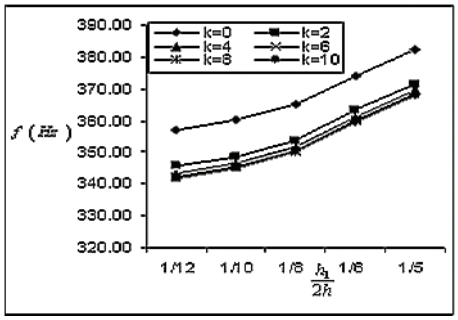

Fig. 9. Effect of piezo layer thickness on the natural frequency - clamped supported boundary condition-(third mode).

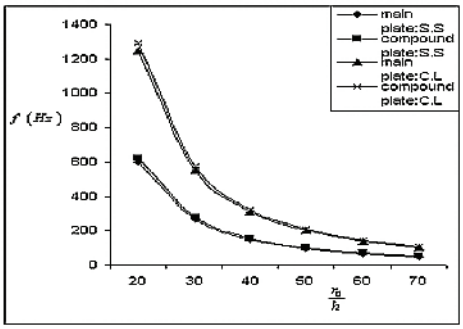

Fig. 10. Effect of aspect ratio r_0/h on the first natural frequency when k=0 under different boundary conditions. (C.L=clamped boundary condition, S.S= simply supported boundary condition)

7. Conclusion

In this paper, the free vibration of a layered FGM plus piezoelectric laminated circular plate based on the classical plate theory is investigated. The properties of FG material changes according to Reddy's model in the direction of plate thickness and distribution of electric potential in the piezoelectric layers follows a quadratic function in short circuited form. The validity of the obtained results for some specific cases was cross-checked with other references as well as by results obtained from FEM solutions. It is further shown that for vibrating circular compound plates with specified dimensions, one can select a specific piezo-FGM plate which can fulfill the designated natural frequency and indeed this subject has many industrial applications.

References

[1] F. E. Crawley and J. Luis, Use of piezoelectric actuators as elements of intelligent structures, *AIAA. J.* 25 (10) (1987) 1373-1385.

[2] T. Takano and H. Hiroshi and T. Yoshro, Analysis of nonaxisymmetric vibration mode piezoelectric annular plate and its application to an ultrasonic motor, *IEEE. Trans on Ultrasonic Ferroelectrics*. 37 (6) (1990) 558-565.

[3] H. Woo-Seok and C. P. Hyun, Finite element modeling of piezoelectric sensors and actuators, *AIAA. J.* 31 (5) (1993) 930-937.

[4] W. Nesbit and J. V. Hagood and J. M. Andrew, Modeling of a piezoelectric rotary ultrasonic motor, *IEEE Trans on Ultrasonic Ferroelectrics.* 42 (2) (1995) 210-224.

[5] P. Heyliger, Exact solutions for simply supported laminated piezoelectric plates, *J. Appl. Mech.* 64 (1997) 299- 306.

[6] J. R. Friend and D. S. Stutts, The dynamics of an annular piezoelectric motor stator, *J. Sound. Vib.* 204 (3) (1997) 421-437.

[7] P. Hagedorn and J. Wallashek, Traveling wave ultrasonic motors part I working principle and mathematical modeling of the stator, *J. Sound. Vib.* 155 (1992) 31-46.

[8] J. Wallashek P. Hagedorn and W. Konrad, 1993 Traveling wave ultrasonic motors part II: a numerical method for the flexural vibrations of the stator, *J. Sound. Vib.* 168 (1993) 115-122.

[9] J. E. Ashton and M. Whitney, *Theory of Laminated Plates*, Stanford, (1970).

[10] R. Szilard, *Theory and analysis of plates-classical and numerical methods*, Englewood Cliffs NJ: Prentice-Hall, (1974).

[11] R. D. Mindlin, Influence of rotary inertia and shear on flexural motions of isotropic elastic plates, *J. Appl Mech. Trans.* ASME E 73 **(**1951) 31-38.

[12] J. N. Reddy, A general third–order nonlinear theory of plates with moderate thickness, *J. Nonlinear Mech.* 25 (1990) 677-686.

[13] J. N. Reddy, A review of refined theories of laminated composite plates, *Shock and Vib Digest*, 22 (7) (1990) 3-17.

[14] A. Nosier and R. K. Kapania and J. N. Reddy, Free vibration analysis of laminated plates using a layer wise theory, *AIAA. J.* 8 **(**1993**)** 2335-2346.

[15] D. Haojiang and et al, Free axisymmetric vibration of transversely isotropic piezoelectric circular plates, *Int. J. Solids Struct.* 36 **(**1999**)** 4629-4652.

[16] H. Deresiewicz and R. D. Mindlin, Axially symmetric flexural vibration of a circular disc, *J. Appl. Mech*. 22 **(**1995**)** 86-88.

[17] H. Deresiewicz, Symmetric flexural vibration of a clamped circular disc, *J. Appl. Mech*. 23 **(**1956**)** 319.

[18] X. Liu and Q. Wang and S. T. Quek, Analytical solution for free vibration of piezoelectric coupled moderately thick circular plates, *Int J. Solids Strut.* 39 **(**2002**)** 2129-2151.

[19] S. Kapuria and P. C. Dumir, Geometrically nonlinear axisymmetric response of thin circular plate under piezoelectric actuation, *J. Sound Vib.* 10 **(**2005**)** 413-4123.

[20] W. H. Duan and S. T. Quek and Q. Wang, Free vibration of piezoelectric coupled thin and thick annular plate, *J. Sound Vib.* 281 **(**2005**)** 119-139.

[21] A. Almajid and M. Taya and S. Hudunt, Analysis of out-of-plane displacement and stress field in a piezocomposite plate with functionally graded microstructure, *Int. J. Solids Struct.* 38 **(**2001**)** 3377-3391.

[22] C. P. Fung, Imperfection sensitivity in the nonlinear vibration of functionally graded plates, *Euro. J. Mech. A/Solids*. 25 **(**2005) 425-4236.

[23] J. J. Hsieh and L. T. Lee, An inverse problem for a functionally graded elliptical plate with large deflection and slightly distributed boundary, *Int. J. Solids Struct.* 43 **(**2006**)** 5981-5993.

[24] T. Parakash and M. Ganapathi, Asymmetric flexural vibration and thermoelastic stability of FGM circular plates using finite element method, *Composite*. B 37 **(**2006**)** 642-649.

[25] J. Yang and S. Kitipornchai and K. M. Liew, Large amplitude vibration of thermo-electro-mechanically stressed FGM laminated plate, *Comput. Meth. Appl. Mech.* 192 (2003) 3861-3885.

[26] Q. Wang and S. T. Quek and X. Liu, Analysis of piezoelectric coupled circular plate, *Smart. Mater. Struct.* 10 (200) 229-239.

[27] D. O. Brush and B. O. Almroth, *Buckling of Bars Plates and Shells*, McGraw-Hill, New York, (1975).

[28] J. N. Reddy, *Theory and Analysis of Elastic Plates*, Taylor and Francis, Philadelphia, (1999).

[29] L. Meirovitch, *Principles and Techniques of Vibrations*, Prentice-Hall, international Inc, (1997).

[30] D. Halliday and R. Resniek, *Physics*, Jhon Wiley and Sons, (1978).

[31] H. F. Tiersten, *Linear Piezoelectric Plate Vibrations*, Plenum press, New York, (1978).

[32] J. N. Reddy and G. N. Praveen, Nonlinear transient thermoelastic analysis of functionally graded ceramic- metal plate, *Int. J. Solids Struct.* 35 **(**1998**)** 4457-4476.

[33] R. C. Wetherhold and S. S. Wang, The use of functionally graded materials to eliminate or control thermal deformation, *Composites Sci Tech.* 6 (1996) 1099-1104.

Saeed Jafari Mehrabadi received his B.S. in mechanical Engineering from Azad University, Arak, Iran, in 1992. He then received his M.S. from Azad University, Tehran, Iran in 1995. Now he is a faculty member of the department of mechanical engineering in Azad university of Arak, Iran and PhD student of Azad University, Science and Research Campus, Pounak, Tehran, Iran. His interests include computational methods and solid mechanics such as vibration, buckling.